Reactive Power Control for Fast-Acting Voltage Regulation of Distributed Wind Turbines Using Reinforcement Learning

Miguel Jimenez-Aparicio
Sandia National Laboratories
Albuquerque, NM, USA

Rachid Darbali-Zamora
Sandia National Laboratories
Albuquerque, NM, USA

2023 IEEE Kansas Power and Energy Conference (KPEC) | 979-8-3503-3540-8/23/$31.00 ©2023 IEEE | DOI: 10.1109/KPEC58008.2023.10215464

***Abstract*—Distribution systems may experience fast voltage swings in the matter of seconds from distributed energy resources, such as Wind Turbines Generators (WTG) and Photovoltaic (PV) inverters, due to their dependency on variable and intermittent wind speed and solar irradiance. This work proposes a WTG reactive power controller for fast voltage regulation. The controller is tested on a simulation model of a real distribution system. Real wind speed, solar irradiation, and load consumption data is used. The controller is based on a Reinforcement-Learning Deep Deterministic Policy Gradient (DDPG) model that determines optimum control actions to avoid significant voltage deviations across the system. The controller has access to voltage measurements at all system buses. Results show that the proposed WTG reactive power controller significantly reduces system-wide voltage deviations across a large number of generation scenarios in order to comply with standardized voltage tolerances.**

***Index Terms*—Voltage Regulation, Wind Turbine Generator, Solar Photovoltaic, Reinforcement Learning**

I. Introduction

The increasing integration of Distributed Energy Resources (DERs) into the distribution grid is paving the way towards a more flexible, resilient and democratized power system. In addition, bringing the generation closer to the consumption have numerous benefits, such as reducing power flows (and losses) in transmission lines, and increasing reliability. However, due to their variability, DERs may cause undesirable effects.

Significant DER penetration may cause noticeable voltage deviations due to sudden power injection changes. DERs' output is subject to intermittent, and often fast-changing, natural resources. For example, clouds can create sudden variations from Photovoltaic (PV) output up to 15% per second [1]. The IEEE 1547 standard observes voltage variations up to 3% per second, on medium voltage, and 5% on low voltage settings [2]. In small geographical areas, these voltage swings may be significant. ANSI standards require that voltage deviations are in the range of $\pm$ 5% for systems operating at less than 600 V, and from -2.5% to +5% at more than 600 V [3].

Voltage regulation on distribution systems has been implemented to maintain system voltages within boundaries under very different system conditions. Traditionally, tap transformers have been one of the main voltage regulation devices at the distribution level. However, in many cases, DERs can respond much faster than transformer taps. The IEEE 1547 standard encourages using DER for voltage control, although the speed (time frame of tens of seconds) and regulation techniques (linear relationship between voltage and reactive power) are significantly below DER capabilities. Power electronic devices offer an unmatched voltage regulation capability as they control reactive and active power injection/absorption independently. According to the IEEE 1547 standard, DERs can offer voltage regulation when the generated active power is larger than 20% of the plant rating. Nevertheless, fast voltage regulation can still be pursued below this threshold [4].

II. Background

Voltage regulation in distribution systems is traditionally achieved using several types of equipment, such as Synchronous Generators (SG), typically located at the substation; capacitor banks, installed by local utilities in certain points to improve power quality (although they produce strong transients that have to be mitigated) [5]; or voltage regulator taps, which introduce time delays of at least tens of seconds [6]. On the other hand, DERs can provide similar reactive power injection (as SG or capacitor banks) or absorption, as long as the fixed apparent power limit is not surpassed [7]. This is detailed in (1):

$$|q| \leq \sqrt{s^2 - p^2} \tag{1}$$

where q refers to the generated reactive power, s is the apparent power limit and p is the injected active power into the system. Changes in reactive power output can be done as fast as cycle-to-cycle time scale. The usage of existing DERs for voltage regulation tackles most of the previously mentioned

"This article has been authored by an employee of National Technology & Engineering Solutions of Sandia, LLC under Contract No. DE-NA0003525 with the U.S. Department of Energy (DOE). The employee owns all right, title and interest in and to the article and is solely responsible for its contents. The United States Government retains and the publisher, by accepting the article for publication, acknowledges that the United States Government retains a non-exclusive, paid-up, irrevocable, world-wide license to publish or reproduce the published form of this article or allow others to do so, for United States Government purposes. The DOE will provide public access to these results of federally sponsored research in accordance with the DOE Public Access Plan https://www.energy.gov/downloads/doe-public-access-plan."

979-8-3503-3540-8/23/$31.00 ©2023 IEEE

Authorized licensed use limited to: Sandia National Laboratories. Downloaded on November 05,2025 at 19:49:10 UTC from IEEE Xplore. Restrictions apply.

problems. Grid-support functions on hybrid systems is a common research topic [8]–[11].

Voltage regulation using solar PV inverters has been largely analyzed. This can be achieved by controlling reactive power injections. One of the most employed is the Volt-Var Curve (VVC) [12]. The VVC locally defines a set of reactive power setpoints that depends on the local node voltage [13]. The larger the voltage deviation, the larger the reactive power injection/absorption. This approach effectively reduces voltage deviations and minimizes system losses.

Regarding voltage regulation using Wind Turbine Generators (WTGs), previous research has been focused on the transmission level. The works in [14], [15] proposes a proportional control to calculate the reactive power setpoint. The control adjusts the WTGs output within 1 second. Furthermore, [16] shows that voltage deviations due to wind speed variations can be largely suppressed using reactive power. On the distribution side, [17] demonstrates that VVC can lead to energy savings. In addition, WTGs using VVC can effectively help to maintain system voltage within limits in case of sudden events [18]. However, the larger the number of elements in the system, the more challenging is to develop efficient controllers. For this reason, many research works rely on Machine-Learning or Deep-Learning techniques on their approaches. For example, [19] proposes a VVC optimization for smart inverters using Reinforcement Learning (RL). Other works trained multiple RL agents for voltage control on distribution systems, using electric vehicles and energy storage systems [20], pumped-storage hydro power [21], or PVs [22]. The dispatch times are 1 hour, 1 hour, and 5 minutes, respectively. The work in [23] creates a multi-agent RL scheme for voltage regulation using PVs and WTGs, with a 5 minutes dispatch interval.

The contribution of this paper is the design, training and validation of a RL agent for voltage regulation using reactive power in distributed WTGs. The proposed controller can regulate on a tight band around nominal voltage, successfully avoiding violations to the ANSI C84.1 standard. Compared to previous literature, the dispatch interval is significantly lowered down to just 50 milliseconds to provide fast voltage regulation in case of sudden PV DER generation changes and load events. Compared to other droop-based approaches, such as VVC, the proposed RL agent is optimized for operating in this system, which ensures a response with greater precision.

III. Methodology

A. System Description

The distribution system is a MATLAB-Simulink model of the Scaled Wind Farm Technology (SWiFT) test site located in Lubbock, Texas [24]. It consists of a microgrid that can be connected to the grid through a substation. The system includes 3 Type-IV WTGs rated at 200 kVA, a variable load rated at a 500 kVA, and a solar PV array rated at 150 kVA [25]. A schematic of the site is shown in Fig. 1. Buses 1 to 9 are rated at medium voltage (12.47 kV), while Bus 10 is low voltage (480 V).

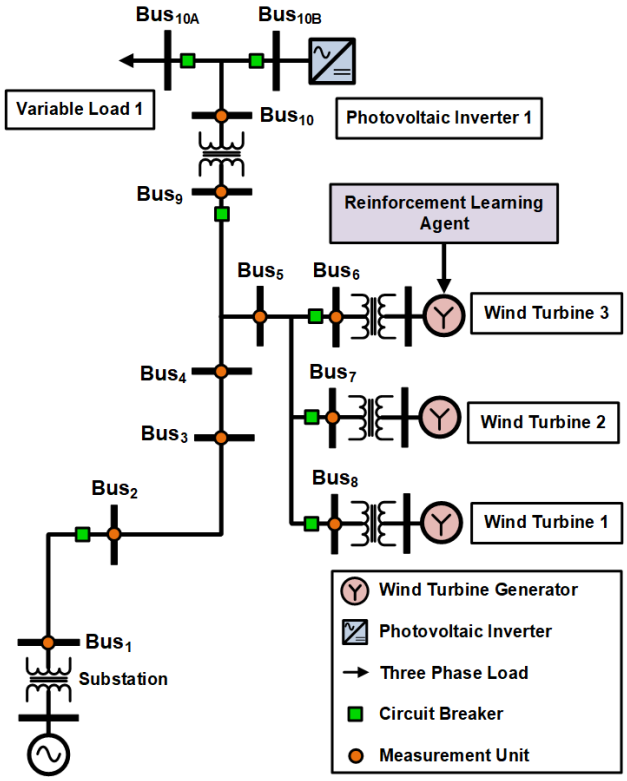

Fig. 1: One-line diagram of SWiFT testing site model.

The WTG models allow commanding the reactive power setpoints of the grid-side converter [26]. The reactive power is limited by the active power and apparent power limit. The proposed RL agent is deployed only on WTG 3. The other WTGs reactive power setpoints are set to zero.

B. Voltage Regulation Controller Algorithm

The proposed WTG controller is based on a RL Deep Deterministic Policy Gradient (DDPG) agent, which generates a reactive power setpoint for WTG 3 every 50 milliseconds. The DDPG agent attempts to provide actions that maximizes the expected long-term reward, which penalizes deviations from the nominal voltage. The ANSI C84.1 standard establishes that system voltages must stay in a range from -2.5% to +5% from nominal voltage ($\pm 5\%$ for Bus 10). To comply with the standard, the DDPG agent will maintain system voltages on a much tighter band: from 0.98 p.u. to 1.02 p.u.

The DDPG agent is composed of four function approximators: the actor $\pi(S, \theta)$, target actor $\pi_t(S_t, \theta_t)$, critic $Q(S, A, \phi)$, and target critic $Q_t(S_t, A_t, \phi_t)$. Respectively, they are composed of the trainable parameters θ, θ_t, ϕ, and ϕ_t. The actor will try to approximate the best policy that maps an observed state S to an optimal control action A. On the other hand, the critic estimates the expectation of the long term reward for such action. The target actor and critic approximators have the same functionality as the main approximators, but they only receive soft updates to increase learning stability. In addition, the DDPG agent has a buffer R that stores past experiences. The agent is updated using a batch of randomly sampled

Authorized licensed use limited to: Sandia National Laboratories. Downloaded on November 05,2025 at 19:49:10 UTC from IEEE Xplore. Restrictions apply.

experiences to increase training stability. During training, the action chosen by the actor is perturbed using a stochastic noise, which promotes exploration.

The continuous observation state S is comprised of 10 observations: the RMS voltage values, in p.u., from Buses 1 to 10. The action is the reactive power setpoint for WTG 3, and it can take any value between [-1, 1] p.u. The reward function $r(S_t, A_t)$ is calculated in every control time step i, and is comprised of the following terms:

$$r_i = -\left[k_A A_i(Q) + k_B B_i(V) + k_C C_i(V) + k_D D_i(V)\right] \quad (2)$$

$$A_i(Q) = |Q_{WTG\,3,i}| \text{ in p.u.} \quad (3)$$

$$B_i(V) = \sum_{b=1}^{10} D_{b,i}$$
$$\text{where } D_{b,i} = \begin{cases} 1, & \text{if } V_{b,i} \notin [0.98, 1.02] \text{ p.u.} \\ 0, & \text{otherwise} \end{cases} \quad (4)$$

$$C_i(V) = \begin{cases} \max(0.98 \text{ p.u.} - V_{b,i}) \text{ for } b = \{1, ..., 10\}, \\ \qquad \text{if } V_{b,i} \leq 0.98 \text{ p.u.} \\ 0, \quad \text{otherwise} \end{cases} \quad (5)$$

$$D_i(V) = \begin{cases} 1, & \text{if } V_{b,i} \notin [0.9, 1.1] \text{ p.u.} \\ 0, & \text{otherwise} \end{cases} \quad (6)$$

where $A_i(Q)$ is the term that penalizes the control effort, $B_i(V)$ is the count of how many voltage signals are out of bounds, $C_i(V)$ tracks the largest under-voltage deviation (if any), and $D_i(V)$ is the exceed bounds condition. The value of the constants from k_A to k_D is: 0.5, 1, 300 and 100, respectively. These values ensure an increasing penalization to to keep as many node voltages withing bounds, while avoiding large nodal under-voltages deviations (as may happen under certain PV generation and load consumption scenarios). The control action is slightly penalized to avoid over-usage.

The critic Q parameter is trained by minimizing the loss L:

$$L = \frac{1}{N} \sum_{i=1}^{N} (y_i - Q(S_i, A_i|\phi))^2 \quad (7)$$

where N is a batch of transitions (S_i, A_i, R_i, S_{i+1}) from R, and y_i is calculated using the Bellman equation:

$$y_i = r_i + \gamma Q_t(S_{i+1}, \pi_t(S_{i+1}|\theta_t)|\phi_t) \quad (8)$$

where γ is the discount factor. The actor policy is updated using the sampled policy gradient:

$$\nabla_\theta J \approx \frac{1}{N} \sum_{i=1}^{N} \nabla_A Q(S_i, A_i|\phi) \nabla_\theta \pi(S_i|\theta) \quad (9)$$

Eventually, the target networks are updated using the smoothing factor τ:

$$\theta_t = \tau\theta + (1-\tau)\theta_t$$
$$\phi_t = \tau\phi + (1-\tau)\phi_t \quad (10)$$

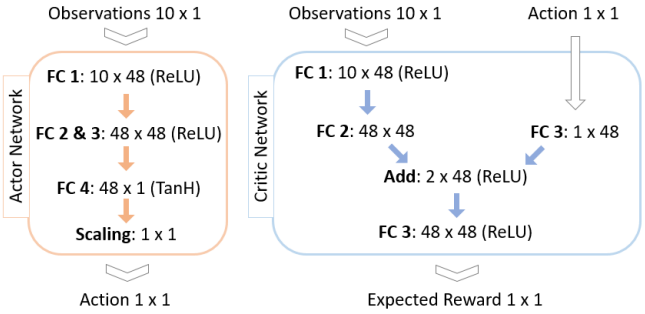

Fig. 2: Actor and critic network structures.

Fig. 2 shows the structure of the actor and critic networks. The actor network is composed of 4 Fully Connected (FC) layers, and a scaling layer. The activation layer is ReLU for FC 1 to 3, and TanH for FC 4. The critic network is composed of two sub-networks, one for the observations (FC 1 and 2) and one for the actor's action (FC 3), which are joined later (FC 4 and 5). The number of neurons on the hidden layers is 48 for both actor and critic network.

C. Training Data

Wind speed, solar irradiance and load consumption data is obtained from the SWiFT site. The length of the data is: 2844, 5000, and 3540 seconds, respectively. The controller is trained over 520 episodes, of 200 seconds each, in which arrays of wind speed, solar irradiation and load consumption are randomly sampled out from the available data.

IV. Results

The DDPG controller is trained using a laptop computer with an Intel Core i9-10885H processor, and 32 GB of RAM. Due to the simulated system complexity, the training takes 10 days (in real time). The averaged reward increase is shown in Fig. 3. Notice that the reward is low in the first hundred episodes due to the agent inexperience and initial exploration.

The results section is divided in two subsections. The first one shows the controller behavior over a span of 400 seconds during a significant PV generation fluctuation. At t = 250 seconds, an unexpected 40% load step takes place at Bus 10. The PV generation and load consumption in the test simulation can be seen in Fig. 4. Wind speed profiles are shown in Fig. 5.

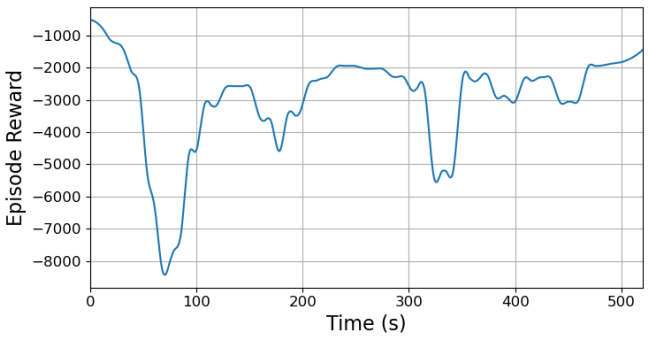

Fig. 3: Averaged reward per episode during training.

Authorized licensed use limited to: Sandia National Laboratories. Downloaded on November 05,2025 at 19:49:10 UTC from IEEE Xplore. Restrictions apply.

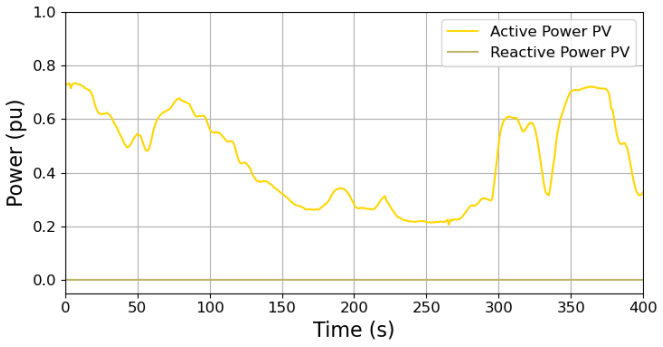

(a)

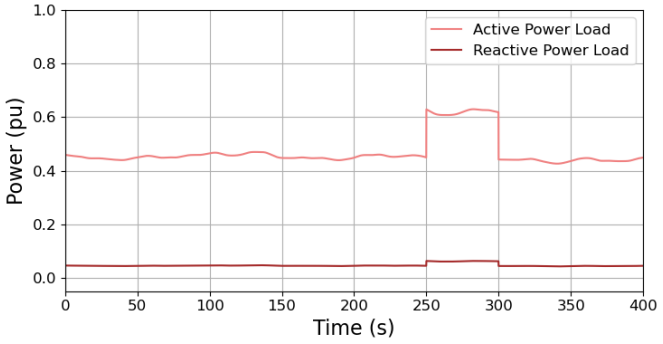

(b)

Fig. 4: Active and reactive power setpoints for devices located at Bus 10. (a) PV (generating). (b) Load (consuming).

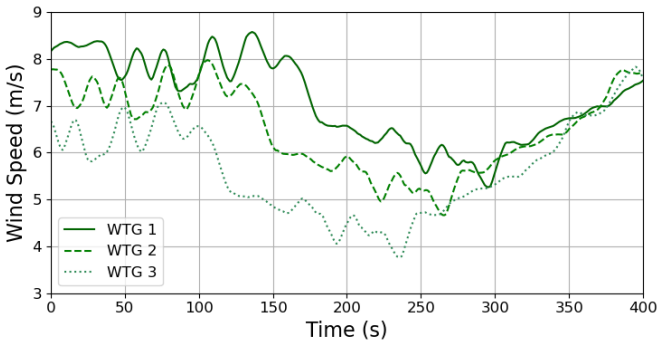

Fig. 5: Wind speed profiles.

To give a deeper understanding of the advantages of using this controller, the second subsection analyzes the voltage deviation reduction over a testing set of 80 additional episodes. The employed system is prone to under-voltage deviations. In order to compare the performance of the proposed controller and the base case, the total under-voltage deviation UV at a simulation time step t is quantified using (11):

$$UV_t = \sum_{b=1}^{10} |0.98 \text{ p.u.} - V_{b,t}| \text{ if } V_{b,t} \leq 0.98 \text{ p.u.} \quad (11)$$

For an episode e of length T_{sim}, an under-voltage score S metric is calculated as:

$$S_e = \frac{1}{T_{sim}} \int_{t=0}^{T_{sim}} UV_t \, dt \quad (12)$$

A. Controller Behavior

Notice that Bus 10, where the load and the PV are connected, is affected by significant voltage swings when the PV generation fluctuates. Note that in the time frame between t = 150 to 300 seconds, the PV power output is significantly low ($<$ 0.3 p.u.). In this scenario of low generation and moderate load consumption, a significant voltage deviation occurs throughout the system (especially at Bus 10). Fig. 6 shows the WTGs output. Fig. 7 shows the system voltages.

The proposed controller's goal is to avoid system-wide voltage deviations outside the range of [0.98, 1.02] p.u.

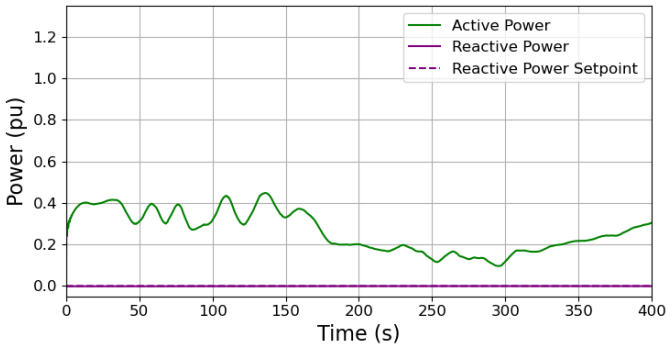

(a)

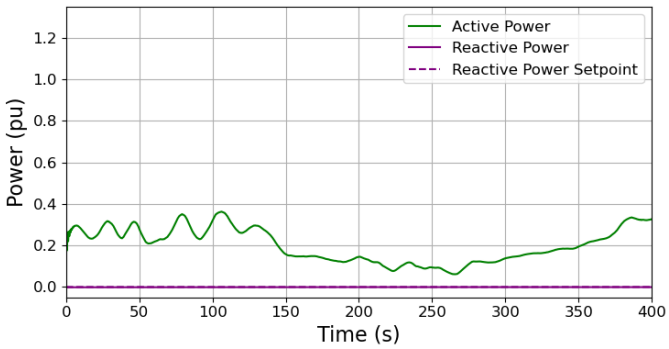

(b)

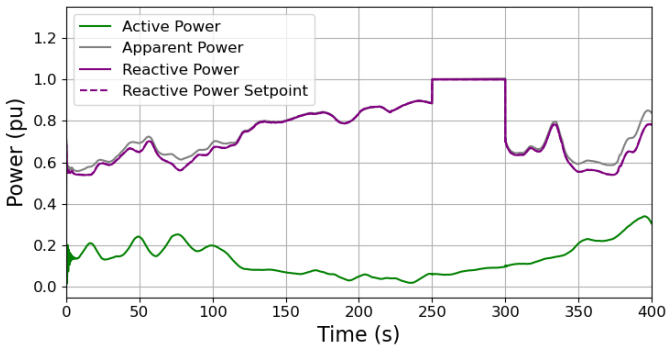

(c)

Fig. 6: WTGs output. (a) WTG 1. (b) WTG 2. (c) WTG 3.

Authorized licensed use limited to: Sandia National Laboratories. Downloaded on November 05,2025 at 19:49:10 UTC from IEEE Xplore. Restrictions apply.

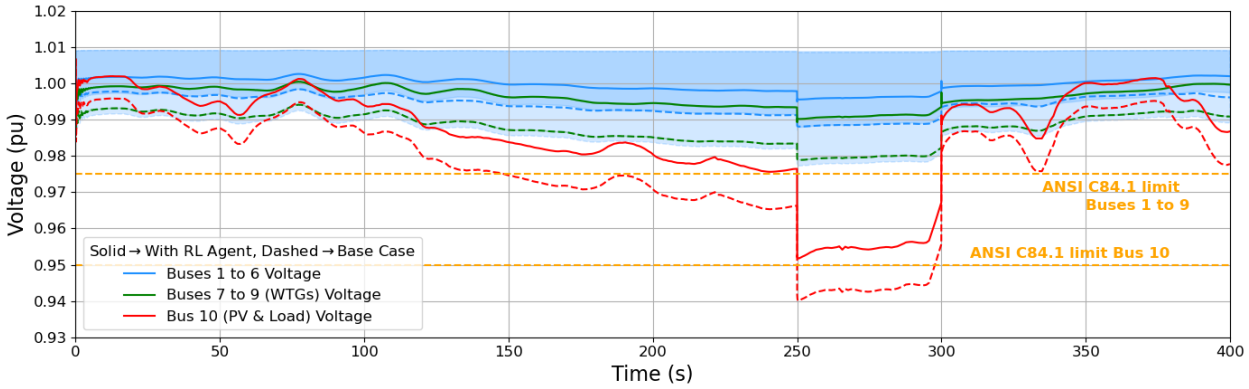

Fig. 7: System voltages comparison with and without the proposed voltage regulation controller.

Through the absorption or injection of reactive power, WTG 3 can regulate the voltage in the system. In this particular test episode, the trained RL agent always commands some reactive power generation to keep voltages close within bounds, as it can appreciated in Fig. 6c. During the episode of low PV generation, the WTG 3 reactive power generation significantly ramps up to almost 0.9 p.u. to dampen the voltage drop. These policy actions are learned over hundreds of simulations under very different DER generation scenarios.

During the sudden load event at t = 250 seconds, the RL agent commands a step in the amount of generated reactive power up to almost 1 p.u. in order to mitigate the sudden voltage drop. The fast dynamics of WTG 3 allows to follow the commanded setpoint immediately. This is supported by a very low WTG 3 active power output ($<$ 0.1. p.u.) due to fairly slow wind speeds. During this period of time, the amount of apparent power never surpasses the limit of 1 p.u.

The benefits of the control on the system voltages can be seen in Fig. 7. The RL agent is trained to avoid large under-voltage deviations below the conservative threshold of 0.98 p.u. The proposed voltage regulation controller successfully mitigates system-wide voltage deviations on the low PV generation scenario. The larger the voltage drop, the larger the reactive power injection. Furthermore, it avoids the violation of the ANSI C84.1 standard from t = 250 to roughly t = 295 seconds. The magnitude of the total under-voltage deviation is calculated by (11). In Fig. 8, it can be observed that the proposed controller significantly reduces the number of under-voltage occurrences and its magnitude.

B. Controller Performance

The performance of the controller on a test set comprised of 80 episodes, 200 seconds each, is analyzed on this section. The RL agent is able to raise system voltages by injecting reactive power to the system. In Fig. 9, it can be seen that bus voltages experience a voltage raise of up to 0.01 p.u. because of the controller's actions. This increase is especially noticeable in the middle and farther buses of the feeder, from the substation point of view. Note that the voltage at Bus 10 in the base case is on average very close to the established 0.98 p.u. lower bound. The voltage at the substation does not significantly see a voltage increase, as this is the point of interconnection with the rest of the grid.

The summary of the controller performance over 80 episodes is displayed on Table I. The RL agent control actions are able to ensure that the score, as calculated in (12), is reduced on a 81.9%: from -0.033 down to -0.006. In addition, the average generated WTG 3 active power per episode P_e is only slightly curtailed: from 0.102 p.u. during the base case, down to 0.100 p.u. using the controller. Results show that the WTG 3's ability to inject Q is heavily employed: the average injected reactive power per episode Q_e is 0.699 p.u.

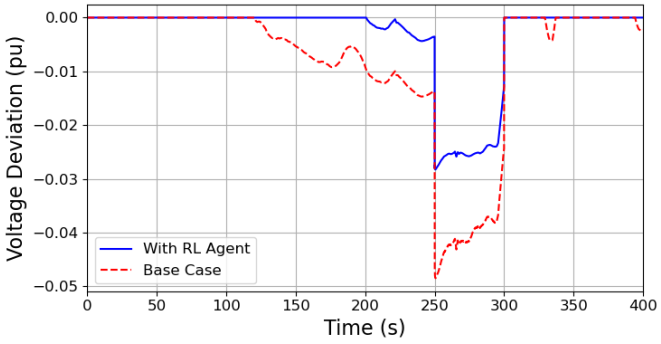

Fig. 8: Total under-voltage deviations below 0.98 p.u.

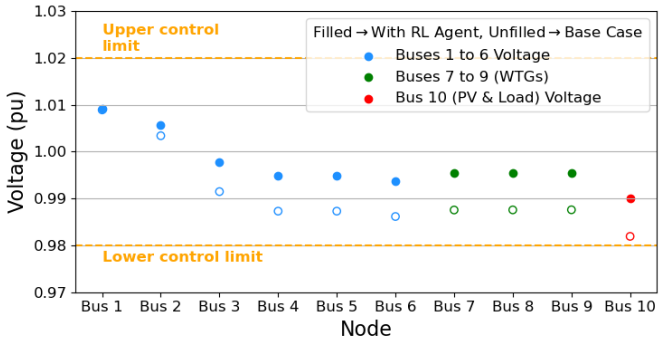

Fig. 9: Mean bus voltages over 80 episodes.

Authorized licensed use limited to: Sandia National Laboratories. Downloaded on November 05,2025 at 19:49:10 UTC from IEEE Xplore. Restrictions apply.

TABLE I: Averaged performance metrics per episode

Use Case	S_e (p.u.)	WTG 3 P_e (p.u.)	WTG 3 Q_e (p.u.)
Base Case	-0.033	0.102	-0.001
With RL Agent	-0.006	0.100	0.699

V. Conclusions

This work proposes a Deep Deterministic Policy Gradient (DDPG) Reinforcement Learning controller for Wind Turbine Generators (WTGs) that performs fast voltage regulation in distribution systems. This is achieved by injecting or absorbing reactive power using the WTG 3 inverter, which has faster dynamics than other voltage regulation equipment. The agent is trained on real data to regulate the voltage within the range from 0.98 p.u. to 1.02 p.u., complying with the ANSI C84.1 standard. The agent's control policy is learned over 520 episodes of 200 seconds each under different scenarios of Photovoltaic (PV) and wind generation, and load consumption. Results on a 400 seconds long test episode show that the proposed DDPG agent significantly reduces voltage deviations due to sudden Distributed Energy Resources (DERs) output swings and unexpected load events. Analyzing the proposed controller's behavior on a test set of 80 episodes, it can be seen that 1) bus voltages in the middle and far-end of the system are raised by about 0.01 p.u., 2) reactive power injection is heavily used (0.7 p.u. in average), and 3) active power generation is just slightly affected.

Acknowledgement

The authors would like to acknowledge the financial support provided by the U.S. Department of Energy (DOE), Office of Energy Efficiency (EERE), Wind Energy Technology Office (WETO) for the Wind Hybrid Integration Platform (WHIP) project under Work Breakdown Structure No. 1.2.6.701 as well as the contributions from Bret Barker and Patrick Gilman.

References

[1] C. Whitaker, J. Newmiller, M. E. Ropp, and B. Norris, "Distributed Photovoltaic Systems Design and Technology Requirements," Sandia Technical Report, SAND2008-0946 P, 2008.

[2] "IEEE Standard for Interconnection and Interoperability of Distributed Energy Resources with Associated Electric Power Systems Interfaces," *IEEE Std 1547-2018 (Revision of IEEE Std 1547-2003)*, pp. 1–138, 2018.

[3] National Electrical Manufacturers Association, *ANSI C84.1-2020 American national standard for electric power systems and equipment : voltage ratings (60 Hz)*. 2020.

[4] D. W. Gao, E. Muljadi, T. Tian, M. Miller, and W. Wang, "Comparison of Standards and Technical Requirements of Grid-Connected Wind Power Plants in China and the United States,"

[5] K. Turitsyn, P. Sulc, S. Backhaus, and M. Chertkov, "Options for Control of Reactive Power by Distributed Photovoltaic Generators," *Proceedings of the IEEE*, vol. 99, no. 6, pp. 1063–1073, 2011.

[6] M. Hartung, E.-M. Baerthlein, and A. Panosyan, "Comparative Study of Tap Changer Control Algorithms for Distribution Networks With High Penetration of Renewables," 2014.

[7] K. Turitsyn, P. Šulc, S. Backhaus, and M. Chertkov, "Distributed control of reactive power flow in a radial distribution circuit with high photovoltaic penetration," in *IEEE PES General Meeting*, pp. 1–6, 2010.

[8] F. Wilches-Bernal, T. Haines, R. Darbali-Zamora, and M. Jiménez-Aparicio, "A Resource Aware Droop Control Strategy for a PV, Wind, and Energy Storage Flexible Power (Flexpower) Plant," in *2022 IEEE Kansas Power and Energy Conference (KPEC)*, pp. 1–5, 2022.

[9] T. Haines, F. Wilches-Bernal, R. Darbali-Zamora, and M. Jiménez-Aparicio, "Flexible Control of Synthetic Inertia in Co-Located Clusters of Inverter-Based Resources," pp. 1–6, 2022.

[10] T. Haines, R. Darbali-Zamora, M. Jiménez-Aparicio, and F. Wilches-Bernal, "The Impact of Co-Located Clusters of Inverter-Based Resources on a Performance-Based Regulation Market Metric," in *2022 North American Power Symposium (NAPS)*, pp. 1–6, 2022.

[11] F. Wilches-Bernal, R. Darbali-Zamora, B. T. Naughton, and J. D. Flicker, "Model characterization and frequency regulation in wind-diesel hybrid microgrids," in *2022 North American Power Symposium (NAPS)*, pp. 1–5, 2022.

[12] J. T. Johnson et. al., "Optimal Distribution System Voltage Regulation using State Estimation and DER Grid-Support Functions,"

[13] A. O'Connell and A. Keane, "Volt–var curves for photovoltaic inverters in distribution systems," *IET Generation, Transmission & Distribution*, vol. 11, no. 3, pp. 730–739, 2017.

[14] N. Cherkaoui, A. Belfqih, F. E. Mariami, J. Boukherouaa, and M. N. Dazahra, "Voltage regulation in the electrical network using reactive power control strategy of WPP based DFIG wind turbine," in *2017 International Conference on Electrical and Information Technologies (ICEIT)*, pp. 1–5, 2017.

[15] S. T. Ojetola, R. Darbali-Zamora, and F. Wilches-Bernal, "An advanced voltage regulation control for distributed wind turbine generators," in *2023 IEEE Power Energy Society Innovative Smart Grid Technologies Conference (ISGT)*, pp. 1–5, 2023.

[16] J. Ouyang, T. Tang, J. Yao, and M. Li, "Active Voltage Control for DFIG-Based Wind Farm Integrated Power System by Coordinating Active and Reactive Powers Under Wind Speed Variations," *IEEE Transactions on Energy Conversion*, vol. 34, no. 3, pp. 1504–1511, 2019.

[17] R. Anilkumar, G. Devriese, and A. K. Srivastava, "Voltage and Reactive Power Control to Maximize the Energy Savings in Power Distribution System With Wind Energy," *IEEE Transactions on Industry Applications*, vol. 54, no. 1, pp. 656–664, 2018.

[18] R. Darbali-Zamora, S. Ojetola, F. Wilches-Bernal, and J. Berg, "Development of a Wind Turbine Generator Volt-Var Curve Control for Voltage Regulation in Grid Connected Systems," 2022.

[19] T. Zhao, Y. Zhang, and M. Yue, "Scalable Deep Reinforcement Learning-based Volt-VAR Optimization in Distribution Systems: a Mean-field Approach," in *2022 IEEE Power Energy Society General Meeting (PESGM)*, pp. 1–5, 2022.

[20] D. Hu, Z. Ye, Y. Gao, Z. Ye, Y. Peng, and N. Yu, "Multi-Agent Deep Reinforcement Learning for Voltage Control With Coordinated Active and Reactive Power Optimization," *IEEE Transactions on Smart Grid*, vol. 13, no. 6, pp. 4873–4886, 2022.

[21] Q. Huang, W. Hu, G. Zhang, D. Cao, Z. Liu, Q. Huang, and Z. Chen, "A novel deep reinforcement learning enabled agent for pumped storage hydro-wind-solar systems voltage control," *IET Renewable Power Generation*, vol. 15, no. 16, pp. 3941–3956, 2021.

[22] D. Cao, W. Hu, J. Zhao, Q. Huang, Z. Chen, and F. Blaabjerg, "A Multi-Agent Deep Reinforcement Learning Based Voltage Regulation Using Coordinated PV Inverters," *IEEE Transactions on Power Systems*, vol. 35, no. 5, pp. 4120–4123, 2020.

[23] D. Hu, Y. Peng, J. Yang, Q. Deng, and T. Cai, "Deep Reinforcement Learning Based Coordinated Voltage Control in Smart Distribution Network," in *2021 International Conference on Power System Technology (POWERCON)*, pp. 1030–1034, 2021.

[24] J. Berg, J. Bryant, B. LeBlanc, D. Maniaci, B. Naughton, J. Paquette, B. Resor, J. White, and D. Kroeker, "Scaled Wind Farm Technology Facility Overview," in *32nd ASME Wind Energy Symposium*, 2014.

[25] R. Darbali-Zamora, F. Wilches-Bernal, and B. Naughton, "Configurable microgrid modelling with multiple distributed energy resources for dynamic system analysis," in *2021 IEEE Power Energy Society General Meeting (PESGM)*, pp. 1–5, 2021.

[26] G. E. North Piegan, R. Darbali-Zamora, and J. C. Berg, "Development and Validation of a Wind Turbine Generator Simulation Model," in *2022 North American Power Symposium (NAPS)*, pp. 1–6, 2022.

Authorized licensed use limited to: Sandia National Laboratories. Downloaded on November 05,2025 at 19:49:10 UTC from IEEE Xplore. Restrictions apply.